Research Article | Vol. 8, No. 7 | 1 Jul 2017 | BIOMEDICAL OPTICS EXPRESS 3458
Biomedical Optics EXPRESS

Detection of Echinococcus granulosus antigen by a quantum dot/porous silicon optical biosensor

YANYU LI,[1] ZHENHONG JIA,[2,*] GUODONG LV,[3] HAO WEN,[3] PENG LI,[1] HONGYAN ZHANG,[1] AND JIAJIA WANG[1]

[1]School of Physical Science and Technology, Xinjiang University, Urumqi 830046, China
[2]College of Information Science and Engineering, Xinjiang University, Urumqi 830046, China
[3]The First Affiliated Hospital of Xinjiang Medical University, Urumqi 830054, China
*jzhh@xju.edu.cn

Abstract: Highly sensitive labeled detection of Echinococcus granulosus using colloidal quantum dots (QDs) based on a porous silicon Bragg mirror sensor are demonstrated. Rabbit anti-p38 labeled CdSe/ZnS QDs was infiltrated in porous silicon pores immobilized Egp38 antigen. QD-antibodies are specifically bound to antigens linked covalently to the pore walls of PSi after the immune reaction. By the design of the transfer matrix method and the preparation of the electrochemical etching method, the fluorescence peak wavelength of the quantum dots is located in the forbidden band of the Bragg mirror. The fluorescence of QDs are enhanced by PSi Bragg mirror. Egp38 antigen detection limit of 300fg/mL is achievable. Our results exhibit that the biosensor combining PSi Bragg mirror and QDs can potentially be applied to the clinical detection of hydatid disease.

OCIS codes: (130.6010) Sensors; (140.4480) Optical amplifiers.

References and links

1. C. Jiang, "Today's regional distribution of echinococcosis in China," Chin. Med. J. (Engl.) **115**(8), 1244–1247 (2002).
2. A. M. C. Restrepo, "The landscape epidemiology of echinococcoses," J. Infect. Dis. Pov. **5**(1), 1–13 (2016).
3. P. Li, Z. Jia, and G. Lü, "Hydatid detection using the near-infrared transmission angular spectra of porous silicon microcavity biosensors," Sci. Rep. **7**, 44798–44815 (2017).
4. N. Massadivanir, ""Optical detection of E. coli bacteria by mesoporous silicon biosensors," J. Vis. Exp. **50805**(81), 1–8 (2013).
5. H. Ouyang, L. A. Delouise, B. L. Miller, and P. M. Fauchet, "Label-free quantitative detection of protein using macroporous silicon photonic bandgap biosensors," Anal. Chem. **79**(4), 1502–1506 (2007).
6. F. A. Harraz, "Porous silicon chemical sensors and biosensors: A review," J. Sens. Actuators B Chem. **202**(10), 897–912 (2014).
7. I. A. Levitsky, "Porous Silicon Structures as Optical Gas Sensors," Sensors (Basel) **15**(8), 19968–19991 (2015).
8. G. A. Rodriguez, J. D. Lonai, R. L. Mernaugh, and S. M. Weiss, "Porous silicon Bloch surface and sub-surface wave structure for simultaneous detection of small and large molecules," Nanoscale Res. Lett. **9**(1), 383 (2014).
9. G. Gaur, D. S. Koktysh, and S. M. Weiss, "Immobilization of Quantum Dots in Nanostructured Porous Silicon Films: Characterizations and Signal Amplification for Dual-Mode Optical Biosensing," J. Adv. Funct. Mater. **23**(29), 3604–3614 (2013).
10. B. Cho, B. Y. Lee, H. C. Kim, H. G. Woo, and H. Sohn, "Fabrication of human IgG sensors based on porous silicon interferometer containing Bragg structures," J. Nanosci. Nanotechnol. **12**(5), 4159–4162 (2012).
11. H. Zhang, Z. Jia, X. Lv, J. Zhou, L. Chen, R. Liu, and J. Ma, "Porous silicon optical microcavity biosensor on silicon-on-insulator wafer for sensitive DNA detection," Biosens. Bioelectron. **44**(1), 89–94 (2013).
12. P. Li, Z. Jia, X. Lü, Y. Liu, X. Ning, J. Mo, and J. Wang, "Spectrometer-free biological detection method using porous silicon microcavity devices," Opt. Express **23**(19), 24626–24633 (2015).
13. A. M. Rossi, L. Wang, V. Reipa, and T. E. Murphy, "Porous silicon biosensor for detection of viruses," Biosens. Bioelectron. **23**(5), 741–745 (2007).
14. F. S. H. Krismastuti, S. Pace, and N. H. Voelcker, "Porous Silicon Resonant Microcavity Biosensor for Matrix Metalloproteinase Detection," J. Adv. Funct. Mater. **24**(23), 3639–3650 (2014).
15. R. P. Haugland, "Handbook of Fluorescent Probes and Research Products," Minerva Farm. **5**(1), 202 (2002).
16. E. Cassette, T. Pons, C. Bouet, M. Helle, L. Bezdetnaya, F. Marchal, and B. Dubertret, "Synthesis and Characterization of Near-Infrared Cu–In–Se/ZnS Core/Shell Quantum Dots for In vivo Imaging," J. Chem. Mater. **22**(22), 6117–6124 (2010).

#296486 https://doi.org/10.1364/BOE.8.003458
Journal © 2017 Received 2 Jun 2017; accepted 18 Jun 2017; published 26 Jun 2017

Biomedical Optics EXPRESS

17. S. J. Lord, H. L. Lee, and W. E. Moerner, "Single-molecule spectroscopy and imaging of biomolecules in living cells," Anal. Chem. **82**(6), 2192–2203 (2010).
18. A. G. Midgett, H. W. Hillhouse, B. K. Hughes, A. J. Nozik, and M. C. Beard, "Flowing versus Static Conditions for Measuring Multiple Exciton Generation in PbSe Quantum Dots," J. Phys. Chem. C **114**(41), 17486–17500 (2010).
19. M. Mazloum-Ardakani, R. Aghaei, and M. M. Heidari, "Quantum-dot biosensor for hybridization and detection of R3500Q mutation of apolipoprotein B-100 gene," Biosens. Bioelectron. **72**, 362–369 (2015).
20. N. H. Nguyen, T. Giang Duong, V. N. Hoang, N. T. Pham, T. C. Dao, and T. N. Pham, "Synthesis and application of quantum dots-based biosensor," J. Adv. Nat. Sci: Nanosci. Nanotechnol. **6**(1), 015015 (2015).
21. X. Tan, S. Liu, Y. Shen, Y. He, and J. Yang, "Quantum dots (QDs) based fluorescence probe for the sensitive determination of kaempferol," Spectrochim. Acta A Mol. Biomol. Spectrosc. **133**(4), 66–72 (2014).
22. C. H. Vannoy, J. Xu, and R. M. Leblanc, "Bioimaging and Self-Assembly of Lysozyme Fibrils Utilizing CdSe/ZnS Quantum Dots," J. Phys. Chem. C **114**(2), 766–773 (2010).
23. A. R. Maity and N. R. Jana, "Chitosan–Cholesterol-Based Cellular Delivery of Anionic Nanoparticles," J. Phys. Chem. C **115**(1), 137–144 (2011).
24. Y. Su, M. Hu, C. Fan, Y. He, Q. Li, W. Li, L. H. Wang, P. Shen, and Q. Huang, "The cytotoxicity of CdTe quantum dots and the relative contributions from released cadmium ions and nanoparticle properties," Biomaterials **31**(18), 4829–4834 (2010).
25. Y. Li, Y. Zhou, H. Y. Wang, S. Perrett, Y. Zhao, Z. Tang, and G. Nie, "Chirality of glutathione surface coating affects the cytotoxicity of quantum dots," Angew. Chem. Int. Ed. Engl. **50**(26), 5860–5864 (2011).
26. D. F. Dorfner, T. Hurlimann, G. Abstreiter, and J. J. Finley, "Optical characterization of silicon on insulator photonic crystal nanocavities infiltrated with colloidal PbS quantum dots," J. Appl. Phys. Lett. **91**(23), 233111 (2007).
27. F. Yang and B. T. Cunningham, "Enhanced quantum dot optical down-conversion using asymmetric 2D photonic crystals," Opt. Express **19**(5), 3908–3918 (2011).
28. C. Liu, Z. Jia, X. Lv, C. Lv, and F. Shi, "Enhancement of QDs' fluorescence based on porous silicon Bragg mirror," J. Phys. B **457**, 263–268 (2015).
29. G. Gaur, "Integrating Colloidal Quantum Dots with Porous Silicon for High Sensitivity Biosensing," J. Proc. MRS. **1301**(15), 463 (2011).
30. S. M. Weiss, "Porous silicon biosensors using quantum dot signal amplifiers," Proc. SPIE. **8594**(3), 859408 (2013).
31. G. L. Johnson and R. Lapadat, "Mitogen-Activated Protein Kinase Pathways Mediated by ERK, JNK, and p38 Protein Kinases," Science **298**(5600), 1911–1912 (2002).
32. E. A. Padlan, "X-ray crystallography of antibodies," Adv. Protein Chem. **49**(1), 57–133 (1996).

1. Introduction

Hydatid disease is a parasitic disease caused by Echinococcus granulosus (also known as tapeworm) that threatens both livestock and humans. Humans are infected by water or vegetables contaminated by excrement of the animal with hydatid disease. Hydatid larvae can damage the body's various organs, especially the liver. In addition to serious harm to human health, hydatid disease also hinders the development of animal husbandry. Hydatid disease is distributed worldwide, and is highly prevalent in western China, such as Xinjiang [1,2]. For hydatid disease, early immunological detection is very important for medical treatment.

There are many methods to detect the biological immune reaction, among which the detection based on porous silicon (PSi) optical sensor is a new method developed in recent years [3–5]. PSi has many advantages, such as large specific surface area, good biological compatibility, easy to be prepared into various optical devices, making it an ideal platform for biosensors [6–8]. There are two main types sensing mechanism of PSi optical sensors for biological detection. The first kind of detection is based on the measurement of refractive index change caused by biological reaction in PSi device. There are several kinds of PSi optical devices, such as PSi single layer [9], multilayer photonic crystal (Bragg reflectors (DBR)) [10], porous silicon microcavity (PSM) which consisted of two DBR and one resonance cavity layer [11]. The biological reaction can be detected by measuring the reflection spectrum shift caused by the refractive index changes of these devices. A spectrometer-free method based on PSi microcavity was developed to measure the refractive index changes with goniometer by the angle spectrum of reflection light. Using this method, label-free biological detection can be realized with high detecting resolution [12]. The second kind of detection is based on the fluorescence changes caused by biological reaction in PSi single layer or PSM. The fluorescence can be derived by a biological molecules, and can also

Biomedical Optics EXPRESS

be emitted from fluorescent dyes which label biological probes or target molecules [13]. The role of PSM is to enhance the fluorescence intensity of the fluorophore embedded within the PSi pores by the photonic structure.

PSi methods based on fluorescence detection are more sensitive than those that detect the refractive index [14]. Typical fluorophores that are used include fluorescein, rhodamine, and boron-dipyrromethene derivatives, and polycyclic aromatic hydrocarbons. However, these molecules have certain drawbacks. For instance, their emission peaks are broad and asymmetric, and are readily photobleached by excitation with a strong laser. Fluorescein derivatives in aqueous solution are sensitive to pH and can be quenched after biological reactions. Rhodamine derivatives have a smaller Stokes radius and thus show spectral overlap, which can prevent the recognition of biological molecules [15]. Polycyclic aromatic hydrocarbon fluorophores absorb light in the ultraviolet spectrum and is carcinogenic, which limits its application as a biological probe.

Quantum dots (QDs) are semiconductor nanoparticles with highly tunable fluorescent properties as a function of both size and shape. QDs have strong fluorescence stability, narrow and symmetrical fluorescence spectra, and are highly resistant to photo-bleaching [16–18]. They also exhibit good biocompatibility and can be chemically modified for labeling or detection of specific biomolecules [19–22]. The QD surface is coated with a layer of nontoxic inorganic or organic molecules or polymers that minimizes their toxicity [23–25].

The fluorescence of QDs can be further enhanced using PSi photonic crystals [26–28]. In recent years, a dual-mode measurement in PSi monolayer film using colloidal QDs has been applied to biological detection [12, 29, 30]. In this study, QDs attached to the target biomolecules serve as signal amplifiers by providing an additional refractive index increase beyond that of the smaller target molecules. The strong fluorescence from the QDs serves as a secondary indication of target molecule attachment in the pores.

Based on the characteristics of the PSi Bragg mirror, we have achieved a highly sensitive biological detection by measuring the fluorescence intensity of QDs attached to the target molecules after biological reaction in this paper. According to the wavelength of the colloidal semiconductor QDs, the PSi Bragg mirror was designed and fabricated. Hydatid antigen (Egp38) was prepared, and immobilized into pores of functionalized PSi. Hydatid antibody (rabbit anti-p38) labeled semiconductor colloidal QDs was linked to target molecules Egp38 after the biological reaction in PSi. The fluorescence intensity of QDs in immune conjugates is almost linear with the concentration of Egp38 antigen. Utilizing the QD/PSi optical biosensor, Egp38 antigen detection limit is 300fg/mL.

2. Materials and methods

2.1 Preparation of Egp38 antigen

A recombinant bacteria pET-28a-Egp38 was cultured firstly, and then the antigen protein was released from the cell by induction and ultrasonic fragmentation. Finally, the antigen Egp38 was obtained by centrifugation and purification (see Appendix).

Biomedical Optics EXPRESS

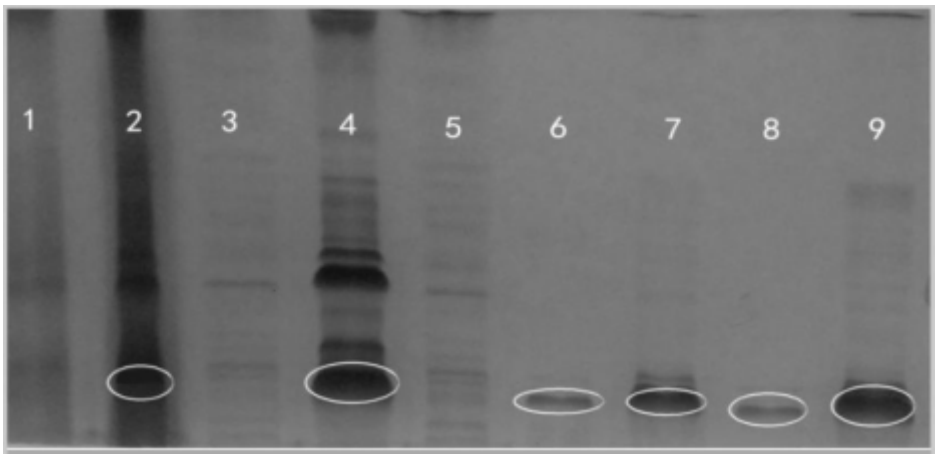

Fig. 1. Egp38 expression as detected by SDS-PAGE. Nine protein samples: 1, before IPTG induction; 2, after IPTG induction; 3, precipitate from ultra-sonication; 4, supernatant after ultrasonication; 5, residual liquid after purification; and protein samples 6–9 (different concentrations of purified Egp38 protein).

The target protein Egp38 was detected in protein Samples 2, 4, and 6–9 by SDS-PAGE (Fig. 1), the protein sample 2 showed that the target protein Egp38 antigen was successfully induced, and the protein sample 4 showed that the target protein was successfully extracted, the 6-9 protein samples showed that the different concentrations of Egp38 antigen.

p38 protein is a class of serine / threonine protein kinases [31], p38 genes in two different developmental stages (protoscolex and adult worm) of Echinococcus granulosus(Xinjiang strain)were expressed, so named for the Egp38. Using the size measurement tool in Swiss-Pdb viewer 4.01 software, the size of Egp38 protein is calculated to be 6.3nm × 4.7nm × 3.4nm.

2.2 QD conjugation with anti-p38 antibody

The molecular weight of Hydatid antibody (rabbit anti-p38) is about 100 kDa, its molecular size can be estimated to about 10nm [32]. 50 µl, 8 µM CdSe/ZnS QD-COOH (Wuhan Jiayuan Quantum Dots Co., Ltd., Wuhan, China) was added to 350 µl PBS for 5 min with continuous stirring at room temperature to give a solution containing 1µM QD-COOH. The diameter of the QD-COOH is about 5nm and the fluorescence peak of the QD-COOH is located at 528nm. QD-COOH were then modified by addition of 30 µL of a 1-ethyl-(3-dimethylaminopropyl) carbodiimide hydrochloride (EDC) solution (10 mg/mL in PBS, pH 7.4) and 30 µL of a sulfo-N-hydroxysulfosuccinimde (NHS) sodium salt solution (10 mg/mL in PBS, pH 7.4) followed by incubation for 30min at room temperature with stirring. EDC and NHS were obtained from the Tianjin Zhiyuan Chemical Reagent Co., Ltd., (Tianjin, China). The derivative QDs were then incubated with 200 µL of rabbit anti-p38 antibody (From The First Affiliated Hospital of Xinjiang Medical University) for 2 h at room temperature with stirring. A 120-µl volume of 5% bovine serum albumin (BSA) was added to the solution; and the reaction allowed to proceed for 2 h at room temperature. The solution was centrifuged to remove any unreacted rabbit anti-p38, BSA, EDC, sulfo-NHS, and QDs and the pellet containing QD-rabbit anti-p38 was dissolved in 600 µl PBS and stored at 4°C.

2.3 Fabrication of PSi photonic device

PSi photonic device with Bragg mirror is designed by the transfer matrix method. The fluorescence of QDs is located on the high reflection band of the PSi Bragg mirror, which can enhance the fluorescence of QDs. Taking into account the functionalization and

Biomedical Optics EXPRESS

immobilization of biomolecules in pores will change the reflection spectrum of the device, we design the central wavelength of the Bragg mirror at 510nm.

PSi samples were fabricated by electrochemical etching of p-type silicon wafers (<100>, 0.03–0.06 Ω cm, boron-doped, Tianjin Semiconductor Technology Research Institute, Tianjin, China) in a mixed solution consisting of 40% hydrogen fluoride (Tianjin Zhiyuan Chemical Reagent Co., Ltd., Tianjin, China) and 98% ethanol (Tianjin Fuyu Fine Chemical Co., Ltd., Tianjin, China) in a volume ratio of 1:1 in the dark. The multi-layer PSi consisted of surface layer and Bragg mirror, as observed by scanning electron microscopy (Fig. 2(A)). A current density of 110 mA/cm^2 was applied for 4 s to form PSi surface layer with the pores diameter of approximately 30 nm and thickness of approximately 780 nm (Fig. 2(B)). QDs labeled biological reactions occur mainly in this layer. The Bragg mirror of the multilayer PSi consisted of a multilayer-stack of alternating high- and low-index films, which was achieved with an etching current density and time of 110 mA/cm^2 for 0.9 s and 40 mA/cm^2 for 1.1 s, respectively. Bragg mirror had 20 layers, the thickness of the high current layer is 120nm and the refractive index is 1.1, the thickness of the low current layer is 90nm and the refractive index is 1.4, the thickness values of two of them are obtained by electron microscope, and the refractive index is calculated by transfer matrix method and the optical thickness formula according to the measured spectral band gap of the PSi, the optical thickness formula of the Bragg mirror: $n_H d_H = n_L d_L = \lambda_c / 4$, the refractive index of the high refractive index layer is nH and nL, respectively, the thickness of the high refractive index layer is dH and dL, respectively, λc is the central wavelength of Bragg mirror. The function of the Bragg mirror is to reflect downward fluorescence from the QDs in first layer. Between the surface layer and the Bragg mirror. A 100-nm-thick PSi layer with small pore was fabricated by applying a current density of 20 mA/cm2 for 0.9 s (Fig. 2(C)). This layer can prevent a part of QDs conjugated with antibody from entering into the mirror and reduce the influence on the optical properties of the Bragg mirror. Etching parameters are controlled by computer, LabVIEW System Design Software, data acquisition card (NI DAQ, CB-68LP) and constant current source (DH1715A-5, Beijing Dahua Radio Instrument Factory, China), Fig. 3 shows the relationship between etching current density and time. The silicon wafers were cleaned in a solution of acetone (Tianjin Zhiyuan Chemical Reagent Co., Ltd., Tianjin, China), ethyl alcohol (Tianjin Zhiyuan Chemical Reagent Co., Ltd,, Tianjin, China), and deionized water by ultrasonication for 10 min before etching.

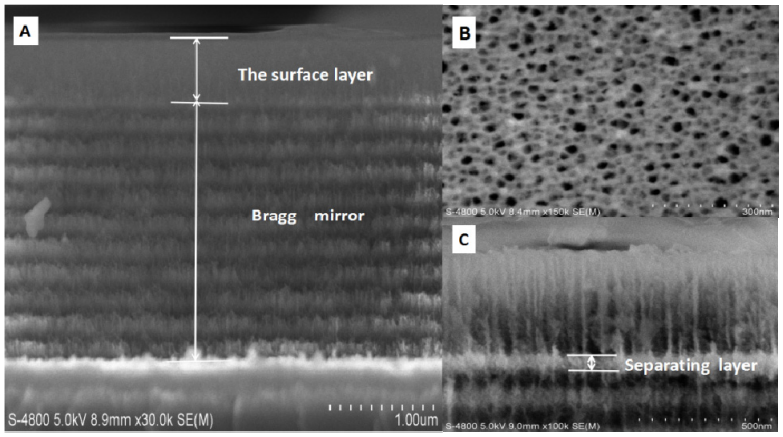

Fig. 2. Scanning electron micrographs showing a cross-sectional view of a multilayer PSi (A), Top view image of the first surface layer (B) and (C) The cross section of pore from multilayer PSi.

Biomedical Optics EXPRESS

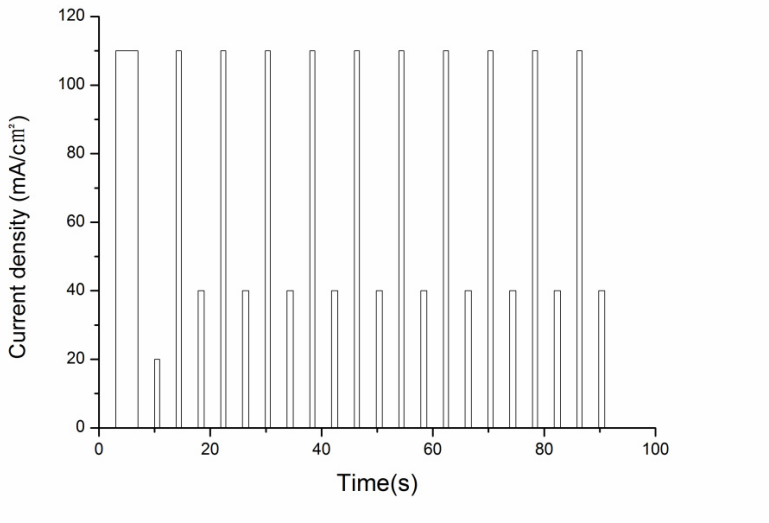

Fig. 3. Scheme of the current density applied in the PSi Bragg mirror etching experiment.

2.4 Functionalization of porous silicon optical device

PSi oxidizes readily when exposed to air, therefore samples were oxidized by immersion in 30% hydrogen peroxide (Tianjin Zhiyuan Chemical Reagent Co., Ltd., Tianjin, China) at room temperature for 24 h to form a SiO_2 layer with characteristic Si-O-Si bonds. The samples were rinsed with ethanol and deionized water and then dried under a stream of nitrogen, and then immersed in a freshly prepared 5% solution of 3-aminopropyltriethoxysilane in deionized water:methanol:APTES (10:10:1) for 1 h. APTES (99%) was obtained from Sigma-Aldrich (St. Louis, MO, USA). The PSi samples were rinsed with ethanol in deionized water and dried under nitrogen gas and then baked in a vacuum drying oven (DZF-6050, Shanghai Yiheng Scientific Instrument Co., Ltd., Shanghai, China) at 100°C for 10 min to increase the cross-link density of APTES molecules and the formation of stable amino groups in PSi. The PSi samples were then soaked for 1 h in deionized water to removed unreacted APTES. After salinization, the PSi samples were immersed in a 2.5% glutaraldehyde solution (19:1, deionized water:50% glutaraldehyde solution) for 1 h at room temperature to immobilize biological molecules in the PSi, then rinsed three times with PBS followed rinsed with deionized water and dried under nitrogen gas. The 50% glutaraldehyde solution was obtained from Aladdin Reagent Co., Ltd. (Shanghai, China).

2.5 Antigen–antibody reaction

The QDs were used as marker to label antibodies by covalent binding, the Egp38 antigen (to be tested) is used to modify PSi. The QD-rabbit anti-p38 is specifically linked with the Egp38 antigen in pores of PSi, the PSi was irradiated by a 370nm wavelength of excitation light, QDs in pores of PSi are excited to emit fluorescence. The Egp38 is quantitatively analyzed by measuring fluorescence intensity of QDs. Figure 4 shows the reaction schematic diagram of the modified PSi with Egp38 antigen and QD-rabbit anti-p38.

Biomedical Optics EXPRESS

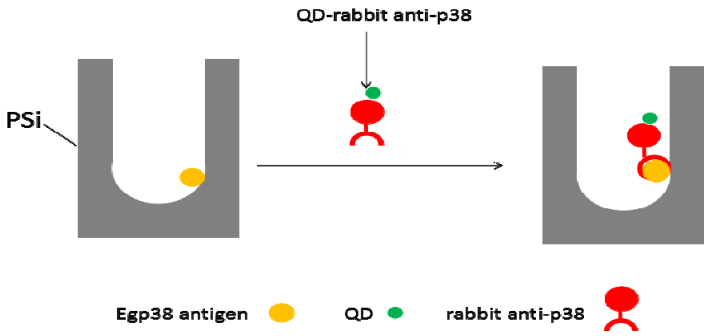

Fig. 4. The reaction schematic diagram of the modified PSi with Egp38 antigen and QD-rabbit anti-p38.

Egp38 antigen with a concentration of 0.5pg/ml was pipetted onto the PSi samples 1–4, and BSA was pipetted onto the PSi sample 5. The five PSi samples were incubated for 2 h at 37°C to ensure that Egp38 molecules were immobilized in PSi, then rinsed with PBS to remove unconjugated antigen and then dried under nitrogen gas. The five PSi samples were incubated with 5% BSA at 37°C for 2h to close any unreacted aldehyde groups and prevent non-specific binding between residual aldehyde groups and the rabbit-anti p38 antibody. This was followed by rinsed with 4-hydroxyethyl piperazine buffer to remove residual BSA followed by rinsed with deionized water and dried under nitrogen gas. PBS, free rabbit anti-p38, free QDs, QD-rabbit anti-p38, QD-rabbit anti-p38 were pipetted onto the five samples, followed by incubation for 2 h at 37°C, rinsed with PBS and deionized water, and dried under nitrogen gas. The reaction conditions and steps are shown in Table 1.

Table 1. Conditions and steps for Egp38 antigen–antibody reaction

Multilayer PSi Sample	Step 1	Step 2	Step 3(various solutions)
1	p38 antigen	5% BSA	PBS
2	p38 antigen	5% BSA	Free Rabbit anti-p38
3	p38 antigen	5% BSA	Free QDs
4	p38 antigen	5% BSA	QDs-Rabbit anti-p38
5	5% BSA	5% BSA	QDs-Rabbit anti-p38

BSA, bovine serum albumin; PBS, phosphate-buffered saline; QD, quantum dot.

We took out a antigen concentration from the protein sample 6-9 and diluted into concentration of 0.5pg/ml, 1pg/ml, 5pg/ml, 10pg/ml, 15pg/ml by PBS. QD-rabbit anti-p38 was added to the modified PSi sensors with five different Egp38 antigen concentrations (0.5, 1, 5, 10, and 15 pg/ml) followed by incubation for 2 h at 37°C. After rinsed with PBS to remove unreacted QD-rabbit anti-p38, PSi samples were rinsed with PBS and deionized water and dried under nitrogen gas.

3. Results and discussion

3.1 Optical properties of QDs and QD-rabbit anti-p38

In this experiment, the CdSe/ZnS QD-COOH is the core shell structure, the ZnS shell can prevent the aggregation of QDs, eliminate the surface states, and avoid the defect state luminescence, so as to improve the luminous efficiency of quantum dots. The fluorescence emission peak of QDs was observed at 528 nm. However, the peak for QDs conjugated with rabbit anti-p38 antibody was shifted to 532 nm owing to covalent coupling between the carboxyl groups of the QD surface and the amino groups of p38 (blue and red lines of Fig. 5). A single antibody molecule can be connected to a number of QDs, which leads to shortening of the distance between QDs, and enhancing in dipole interactions between particles,

Biomedical Optics EXPRESS

increasing shift of Stokes as well as a red shift in the fluorescence spectrum. The decrease of fluorescence intensity could be due to quenching of the protein, it is possible that the positively charged antibody is easily to combine with negatively charged QDs, electron transfer between antibody and QDs, which lead to QDs fluorescence quenching. The fluorescence emission spectrum of QD-rabbit anti-p38 was narrow and symmetrical, indicating that the conjugate had good dispersion.

The reflection spectrum of PSi Bragg mirror is measured by UV-vis spectrophotometer (Hitachi U –4100). The high reflection band center position of Egp38 antigen modified PSi is located at 530nm, the wavelength range of PSi high reflection band is from 470nm to 570nm, which contains the fluorescence peak of QD-rabbit anti-p38 (blue and black lines of Fig. 5), the fluorescence peak of QD is located at the high reflection band of multilayer PSi, and the high reflection band of the PSi Bragg mirror can reflect the fluorescence of QDs that emits downward, which enhances the outward fluorescence from surface of the PSi Bragg mirror [28].

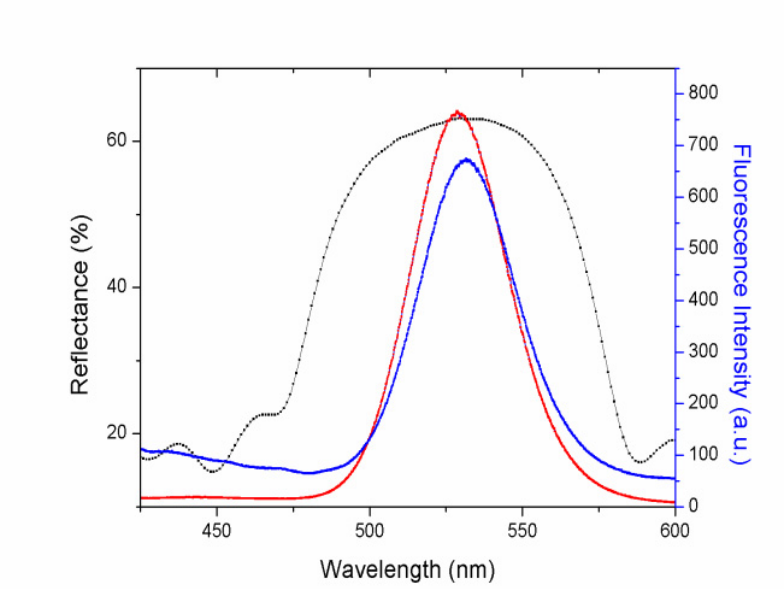

Fig. 5. Fluorescence emission spectra of QDs (red) and QD-rabbi anti-p38 (blue); peaks were visible at around 528 and 532 nm, respectively. The reflection spectrum of PSi (black) after functionalization and immobilization of biomolecules.

3.2 Specificity of the antigen–antibody reaction

The fluorescence intensity of QDs in PSi was measured by the fluorescence spectrometer (Hitachi F-4600, Japan), the excitation wavelength is 370nm. The PSi modified with Egp38 antigen did not produce a fluorescent signal. However, when QD-rabbit anti-p38 was added to the PSi modified with Egp38 antigen a significant fluorescent signal was generated, in contrast the addition of PBS, free rabbit anti-p38 solution, or free QDs, did not generate a fluorescent signal. only PSi sample 4 (QD-rabbit anti-p38 pipetted onto PSi modified with Egp38 antigen) showed a fluorescence signal (Fig. 6), indicating that QD-rabbit anti-p38 was specifically linked to the Egp38 antigen-modified PSi biosensor. The fact that the PBS pipetted onto PSi sample 1 showed no fluorescence indicated that there was no background signal interference. No fluorescence was visible when rabbit anti-p38 without QD was pipetted onto the Egp38 antigen-modified PSi sample 2, but it was not possible to directly observe whether there was a specific antigen–antibody reaction. After cleaning the PSi sample 3 showed no fluorescence demonstrated that free QDs could not be specifically linked

Biomedical Optics EXPRESS

to Egp38 antigen-modified PSi. Finally, the absence of fluorescence for PSi sample 5 showed that QD-rabbit anti-p38 did not link to PSi lacking the biological reaction. Therefore, only when the QD-rabbit anti-p38 reacted with the Egp38 antigen linked pore wall in PSi, the PSi sensor will produce the fluorescent signal.

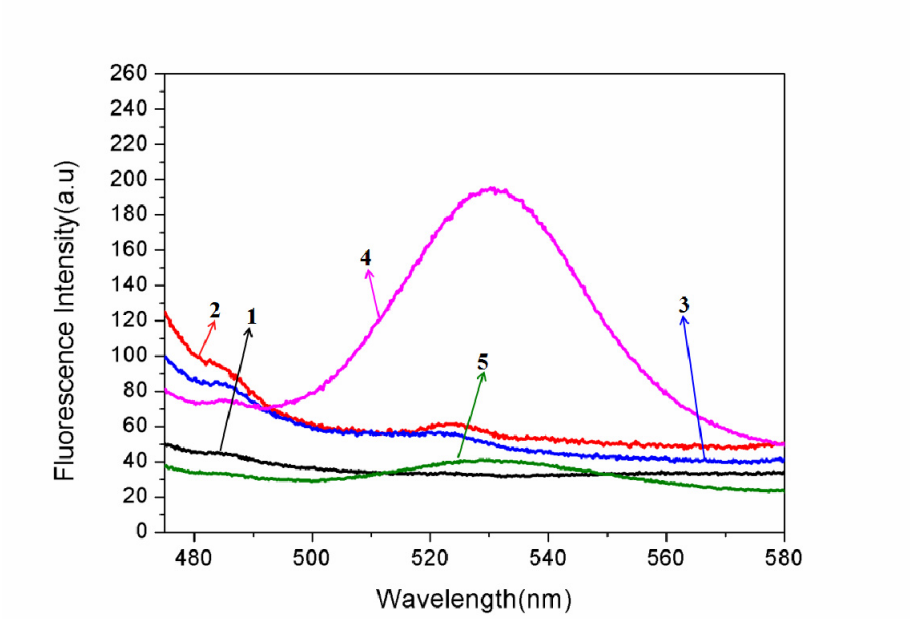

Fig. 6. Fluorescence intensity of QD conjugates under different conditions: 1. the multilayer PSi modified with Egp38 + PBS; 2.the multilayer PSi modified with Egp38 + rabbit anti-p38; 3. the multilayer PSi modified with Egp38 + free QDs; 4. the multilayer PSi modified with Egp38 + QD-rabbit anti-p38; 5. the multilayer PSi modified with BSA + QD-rabbit anti-p38.

The QD-rabbit anti-p38 was pipetted onto the multilayer PSi samples modified with different concentrations of Egp38 antigen. The fluorescence intensity of QD conjugates increased as a function of the Egp38 concentration in the PSi (Fig. 7), reflecting an increase in the number of QD-rabbit anti-p38 antibodies linked to PSi. In this study, we elected to use PSi as a substrate for two main reasons. First, the high reflection band of the PSi Bragg mirror can enhance the fluorescence intensity of QD conjugates and thereby improve detection sensitivity. Second, unreacted QD-rabbit anti-p38 could be easily removed by washing to prevent interference with the fluorescent signal from QD-rabbit anti-p38 that were not linked to PSi. The fluorescence intensity increases with the antigen concentration, and the linear relationship is found at low concentration. The fluorescence intensity of QD conjugates showed a good linear relationship between Egp38 antigen concentrations of 0.5 and 15 pg/ml (Fig. 8) and a high correlation coefficient of 0.998. The detection limit of the QD/PSi optical biosensor was determined to be 300 fg/ml.

Biomedical Optics EXPRESS

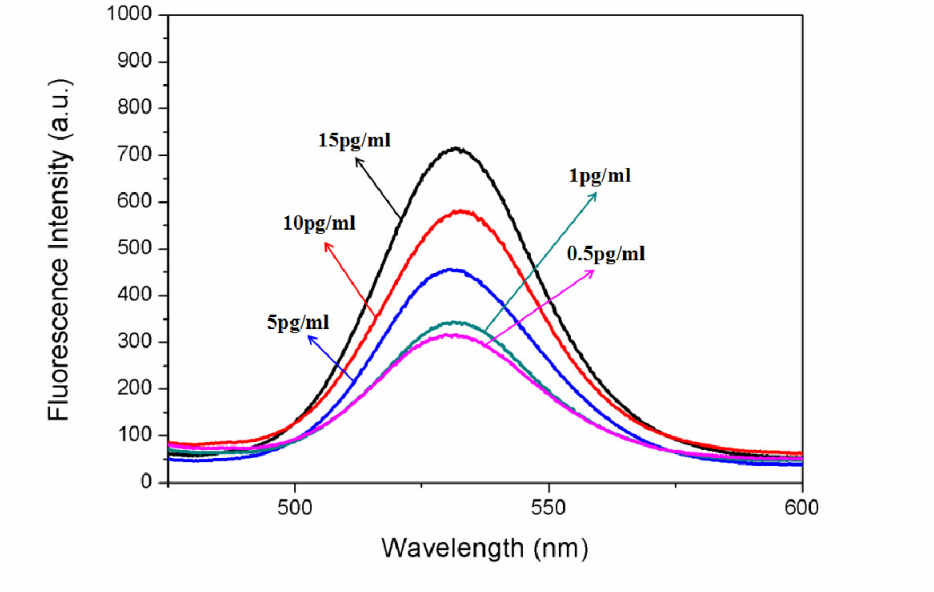

Fig. 7. Image of fluorescence signal after binding of QD-rabbit anti-p38 and Egp38-modified PSi at various concentrations.

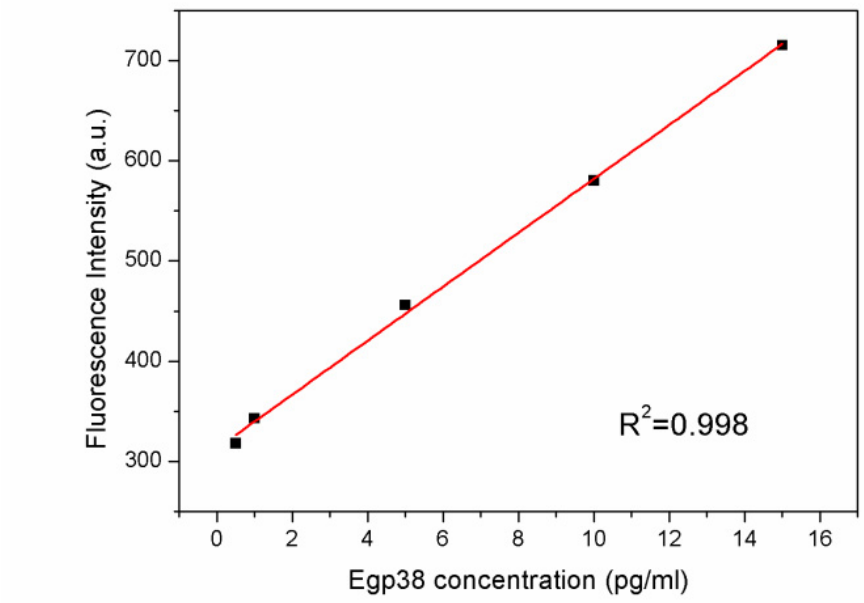

Fig. 8. Detection of Egp38 antigen fluorescence.

3. Conclusions

In this study, a biosensor was fabricated by combining PSi Bragg mirror and QDs to detect Echinococcus granulosus antigen. The biosensor was specific and highly sensitive, with a

Biomedical Optics EXPRESS

detection limit of 300 fg/ml. These findings demonstrate that the biosensor can be used to detect Echinococcus granulosus in clinical specimens for early diagnosis of Hydatid disease; moreover, this system can potentially be modified to detect antigens from other organisms, thereby broadening its applicability.

Appendix

A recombinant bacteria pET-28a-Egp38 was cultured in 10 ml of Luria–Bertani (LB) medium (Beijing Reagan Biological Technology Co., Ltd., Beijing, China) containing 100 mg/ml kanamycin (Beijing Reagan Biological Technology Co., Ltd., Beijing, China) for 12 h at 37°C with shaking. The following day, 2% of the total volume was inoculated in LB medium with the same concentration of kanamycin and cultured for 3 h at 37°C. A 1-ml volume of culture was removed and designated as protein sample 1 (pre-induction). Isopropyl-β-d-thiogalactopyranoside (Promega Biological Technology Co., Ltd., Beijing, China) at a final concentration of 0.1 mmol/l was added to the culture, followed by incubation for 3 h at 27°C with shaking, and a 1-ml volume of culture was removed and designated as protein sample 2. The culture was centrifuged at 8000 r/min at 4°C for 10 min, the supernatant was removed and the cell pellet was washed by two rounds of centrifugation with pre-cooled phosphate-buffered saline (PBS) (Shanghai Sangon Biotech Co., Ltd., Shanghai, China). The cell pellet was re-suspended in pre-cooled PBS, then frozen in liquid nitrogen until use. The re-suspended cell pellets were thawed on ice and a solution of 1% Triton X-100 (Shanghai Sangon Biotech Co., Ltd., Shanghai, China), 1 μM/l of phenylmethylsulfonyl fluoride (Promega Biological Technology Co., Ltd. Beijing, China), and 1 g/l lysozyme (Shanghai Sangon Biotech Co., Ltd., Shanghai, China) was added. The re-suspended cell pellets were sonicated for 30 min at 4°C, the precipitation and supernatant (containing the recombinant protein) were obtained by centrifugation were designated protein samples 3 and 4 respectively.

The recombinant protein was purified using Ni-NTA-His-Bind resin (Novagen, Madison, WI, USA) according to the manufacturer's instructions. Briefly, the equilibrated column containing His-Ni agarose resin was washed overnight with pure water, and the binding buffer was added to the equilibrated column at 4°C, the supernatant was applied to the Ni-NTA-His-Bind resin, the flow through the supernatant was collected and the step was performed a total three times to ensure maximal binding of the recombinant protein to the Ni-NTA-His-Bind resin, the final remaining supernatant was designated as protein sample 5. The Ni-NTA-His-Bind resin was washed three times with wash buffer to remove unbound protein, and the target protein (p38) was eluted with elution buffer containing 250 mM iminazole (Jiangsu Baolai Biotechnology Co., Ltd., Jiangsu, China). Four 1-ml protein samples (nos. 6–9) containing the purified recombinant Egp38 were collected and stored at −80°C.

A 10-μl volume of 4× SDS-PAGE loading buffer was added to each 30-μl protein sample and the mixture at 100 °C for 10 min, followed by centrifugation at 12,000 r/min for 3min. The 12% separating gel (5 ml) consisted of 1.6 ml of 30% acrylamide (Shanghai Sangon Biotech Co., Ltd., Shanghai, China), 2 ml of 1.5 M Tris-HCl (pH 8.8), 1.3 ml of 10% SDS (Shanghai Sangon Biotech Co., Ltd., Shanghai, China), 0.05 ml of 10% ammonium persulfate (Qcbio Science & Technologies Co., Ltd., Shanghai, China), and 1.6 ml H2O. The 5% stacking gel (2 ml) consisted of 1.4 ml H2O, 0.33 ml of 30% acrylamide, 0.25 ml of 1.0 M Tris-HCl (pH 6.8), 0.002 ml of 10% SDS, and 0.002 ml of 10% ammonium persulfate. The 12% separating gel was formed and injected the stacking gel immediately, the stacking gel was allowed to polymerize for 30 min, then was loaded with nine protein samples: 1, before IPTG induction; 2, after IPTG induction; 3, precipitate from ultra-sonication; 4, supernatant after ultrasonication; 5, residual liquid after purification; and protein samples 6–9 (different concentrations of purified Egp38 protein). After protein separation, the separating gel was stained with Coomassie Brilliant Blue R250 solution for 4 h with shaking.

Biomedical Optics EXPRESS

Acknowledgments

This work is supported by the National Science Foundation (NSF) (61575168, 11504313, 61665011), Xinjiang Science and Technology Project (No. 201412112).